Electronic Supplementary Material (ESI) for Journal of Materials Chemistry C.

Simultaneous High Efficiency/CRI/Spectral Stability and Low Efficiency Roll-Off Hybrid White Organic Light-Emitting Diodes by Simply Inserting Ultrathin Red/Green Phosphorescent Emitters in Blue Exciplex

Yuwen Chen, Yibing Wu, Chengwei Lin, Yanfeng Dai, Qian Sun, Dezhi Yang, Xianfeng Qiao and Dongge Ma*

Institute of Polymer Optoelectronic Materials and Devices, Guangdong Provincial Key Laboratory of Luminescence from Molecular Aggregates , State Key Laboratory of Luminescent Materials and Devices, South China University of Technology, Guangzhou, Guangdong 510640, P. R. China

E-mail: msdgma@scut.edu.cn

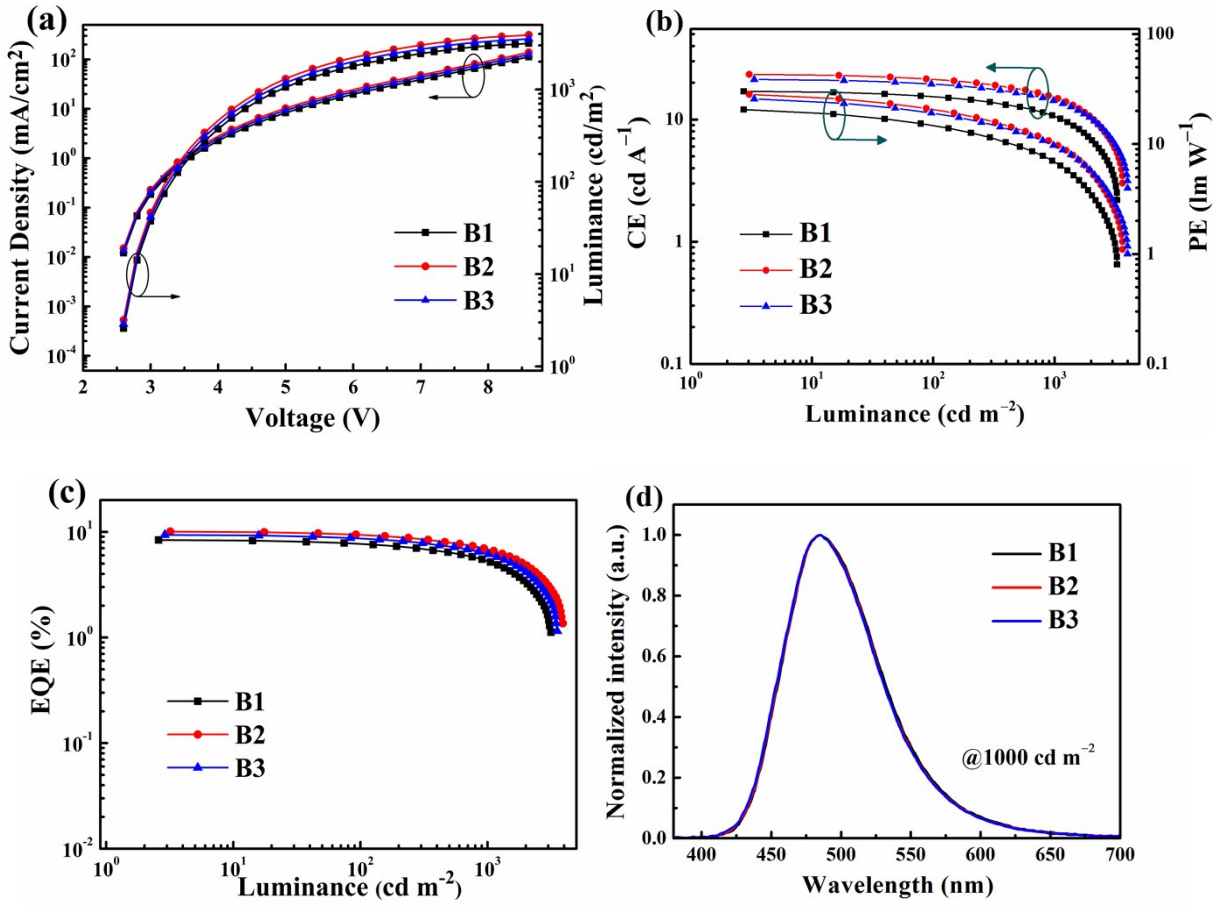

Fig. S1 (a) J−V−L, (b) CE−L−PE, (c) EQE−L characteristics of devices B1, B2 and B3. (d) EL spectra of devices B1, B2 and B3 at the luminance of 1000 cd m^{-2}.

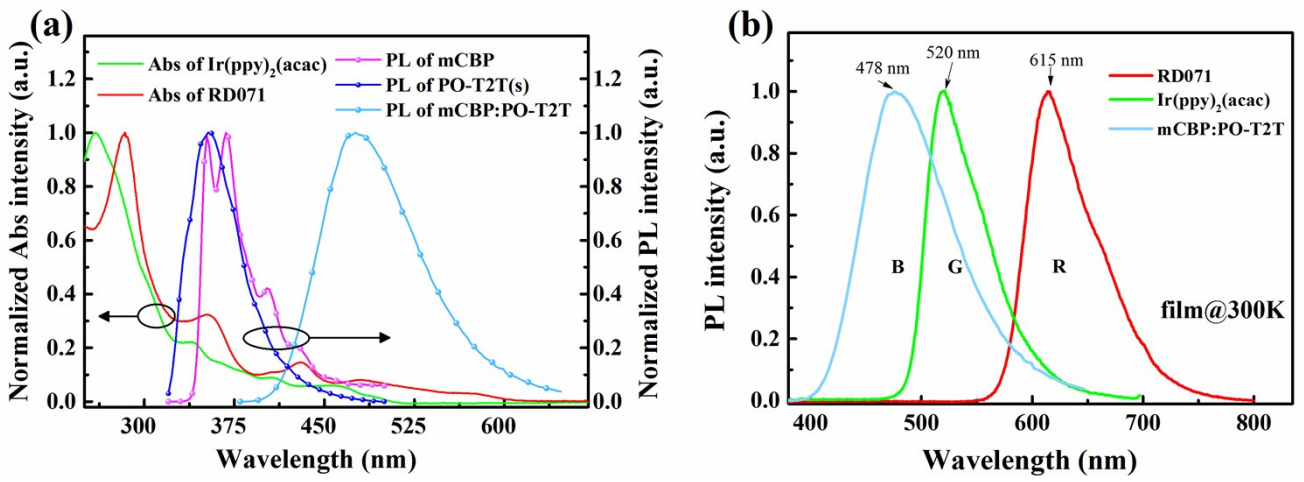

Fig. S2 Photophysical properties of the used organic materials. (a) Absorption spectra of $Ir(ppy)_2(acac)$ and RD071 and PL spectra of mCBP, POT2T and exciplex formed by mCBP and POT2T (1:1, by weight) at 300 K. (b) PL spectra of the neat films of blue emitter and two phosphors (all the neat films are 15 nm thick).

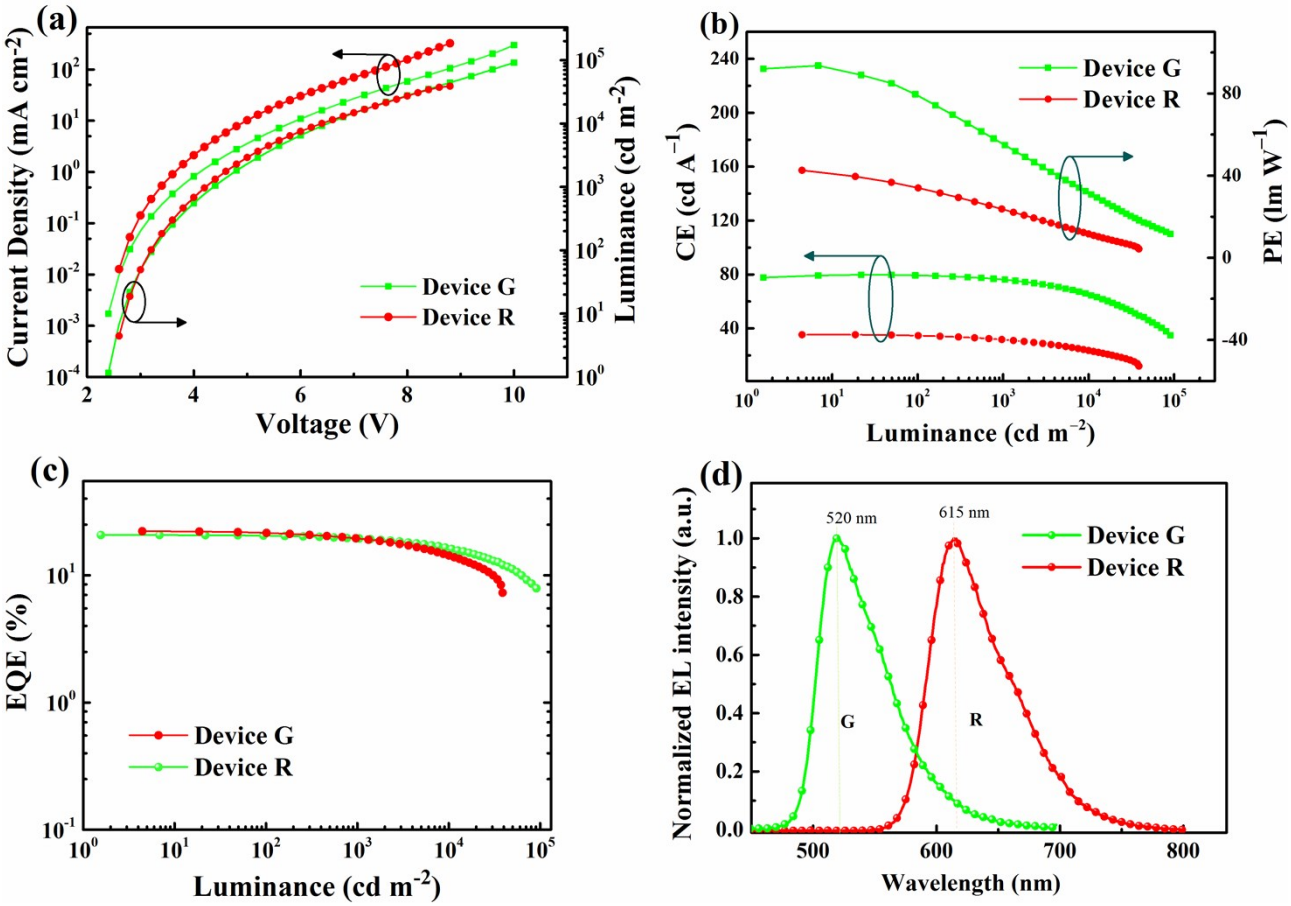

Fig. S3 (a) J−V−L, (b) CE−L−PE and (c) EQE−L characteristics of devices G and R. (d) EL spectra of devices G and R at the luminance of 1000 cd m^{-2}.

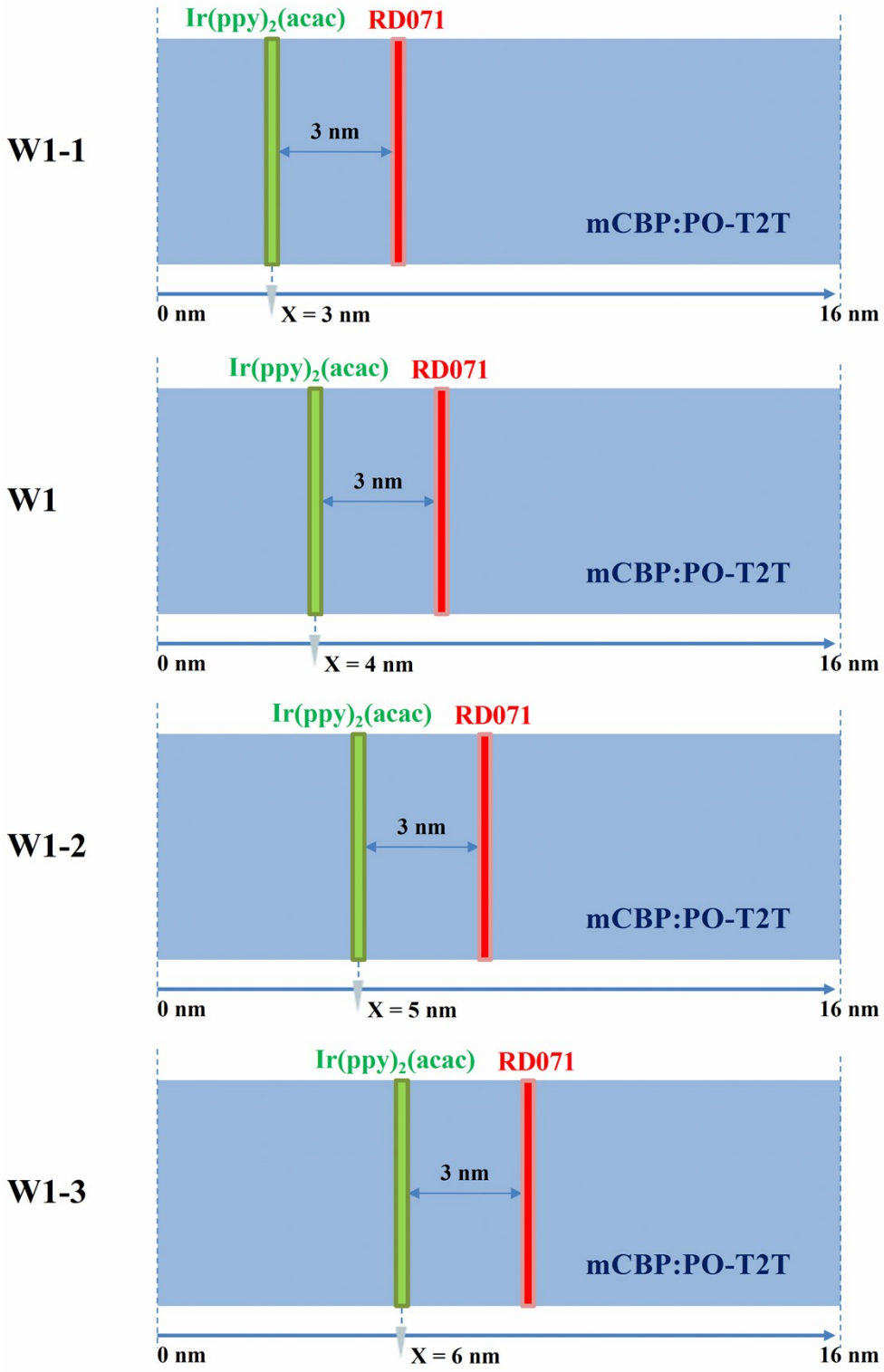

Fig. S4 Schematic diagrams of the positions of phosphorescent UTLs in EML in the fabricated hybrid WOLEDs (W1-1, W1, W1-2 and W1-3).

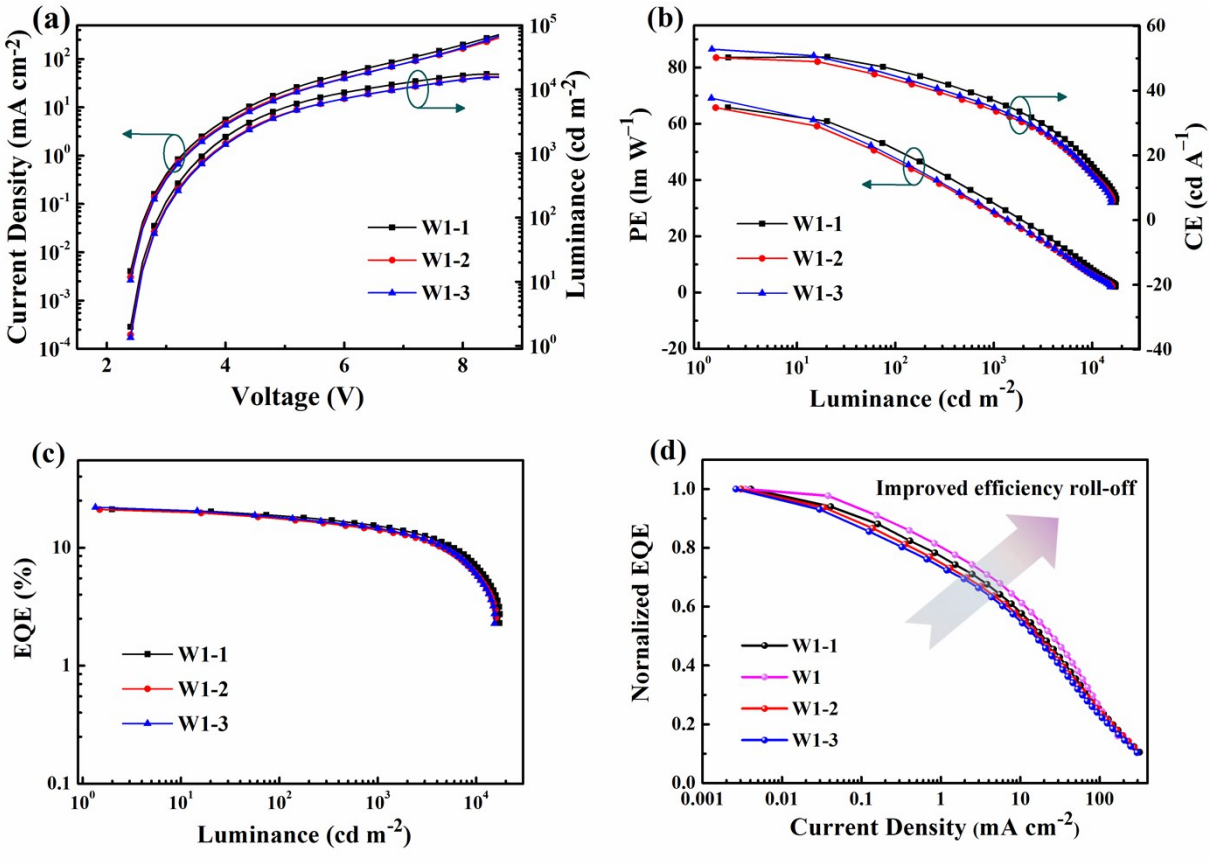

Fig. S5 (a) J−V−L, (b) CE−L−PE, (c) EQE−L and (d) normalized EQE-J characteristics of the resulting four hybrid WOLEDs.

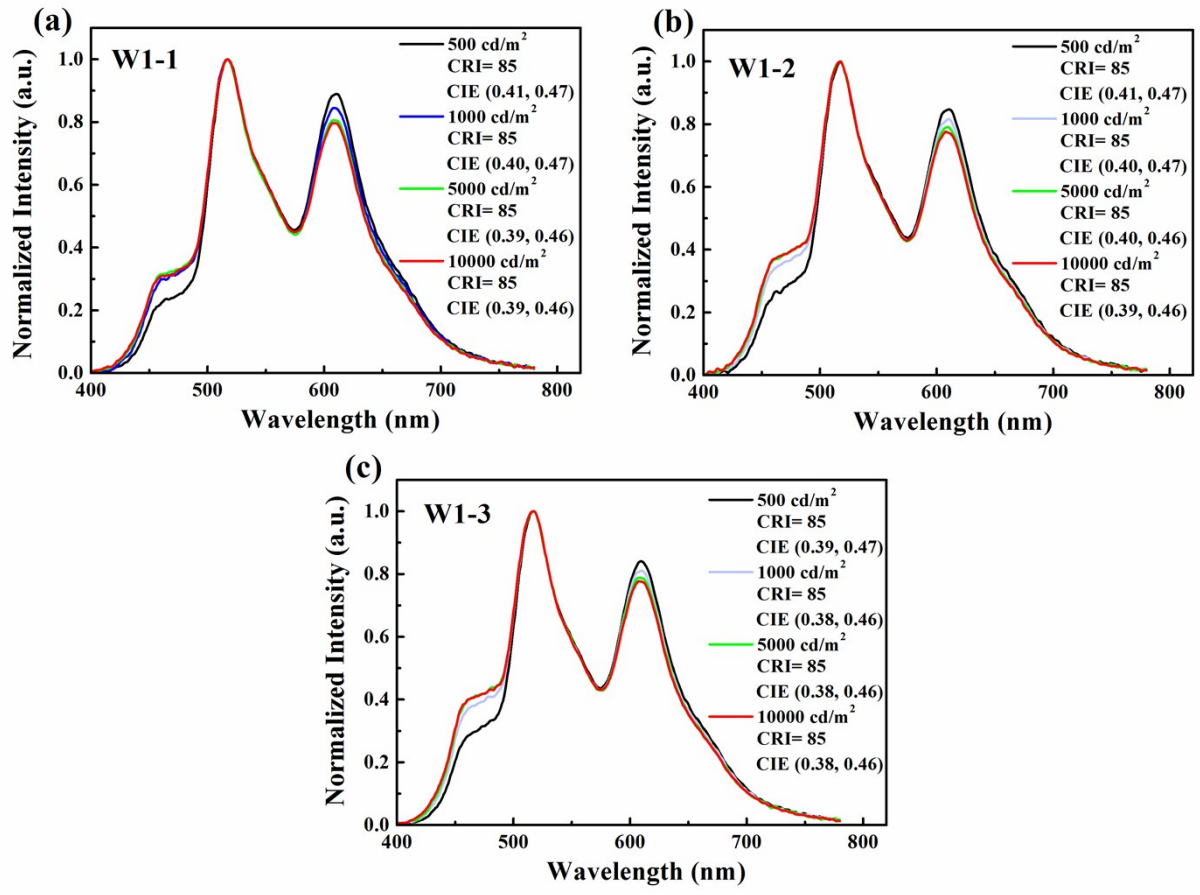

Fig. S6 EL spectra of devices (a) W1-1, (b) W1-2 and (c) W1-3 at different luminance. The inset shows CIE coordinates and CRIs of the corresponding devices at different luminance.

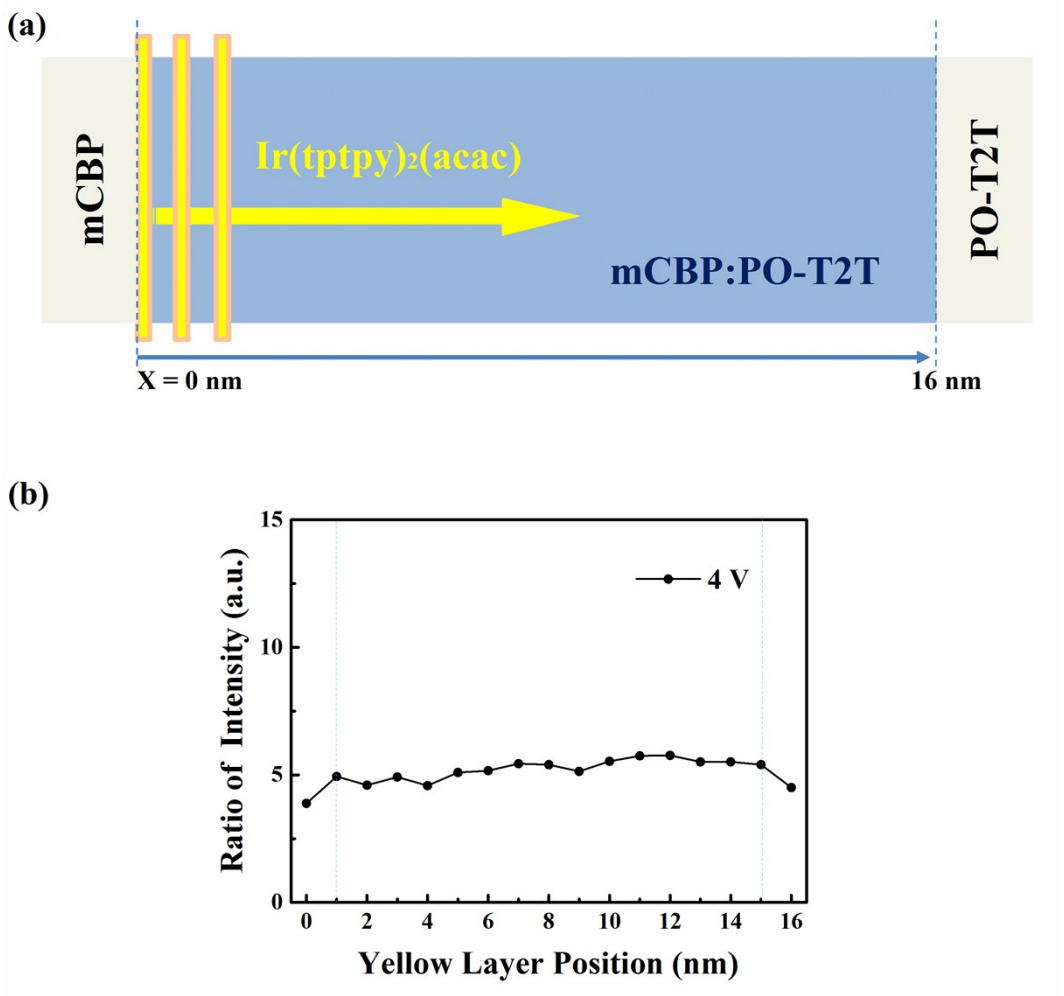

Fig. S7 (a) Schematic diagram of the exploration on exciton distribution in device W1. (b) Relative emission peak intensities of $Ir(tptpy)_2(acac)$ to mCBP:PO-T2T exciplex as a function of the $Ir(tptpy)_2(acac)$ ultrathin layer position in corresponding devices at 4 V. The position of the interlayer between mCBP and mCBP:PO-T2T was recorded as 0 nm.

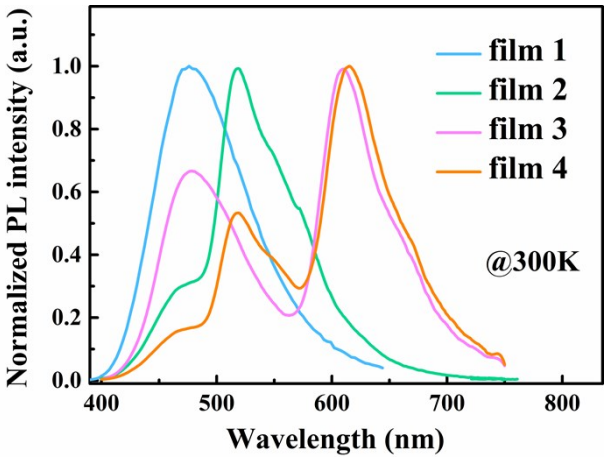

Fig. S8 PL spectra of four different films 1, 2, 3 and 4.

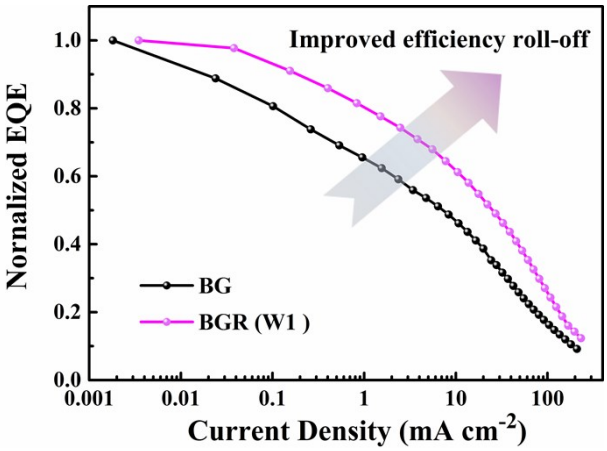

Fig. S9 Normalized EQE-J characteristics of devices BG and BGR (W1).

Table S1. Summary of EL performances of the optimized monochromatic OLEDs.

Device	V_{on}[a] [V]	Max EQE[b] [%]	Max CE[b] [cd A^{-1}]	Max PE[b] [lm W^{-1}]	CIE[c] (x, y)	EQE[c] [%]	CE[c] [cd A^{-1}]	PE[c] [lm W^{-1}]
B1	2.6	8.3	17.1	20.6	(0.15,0.28)	5.2	10.2	6.4
B2	2.6	10.1	23.4	28.2	(0.15,0.28)	7.1	14.7	9.7
B3	2.6	9.3	21.2	25.7	(0.15,0.28)	6.1	13.5	8.8
G	2.4	20.7	77.2	91.6	(0.31,0.62)	19.5	70.1	52.5
R	2.6	21.3	31.3	35.6	(0.64,0.35)	17.9	26.2	19.1

[a] At a luminance of 1 cd m^{-2}, [b] The maximum efficiencies, [c] Measured at 1000 cd m^{-2}.

Supplementary Notes 1:

To study the exciton distribution in mCBP:PO-T2T exciplex emissive layer, here we used an ultrathin phosphorescent sensor (0.06 nm) to ensure that the insertion of the sensing strip does not vastly influence the charge transport. iridium(III)bis(4-(4-t-butyl-phenyl)thieno[3,2-c]pyridinato-N,C2′)acetylacet-onate [$Ir(tptpy)_2(acac)$] was chosen as the sensing layer because it has a very low triplet energy level of 2.2 eV, and the relative emission intensity can provide some information about the exciton spatial distribution. We explored the exciton density profile in device W1 by using the structure of ITO/HATCN (15 nm)/TAPC (60 nm)/TCTA (5 nm)/mCBP (5 nm)/mCBP:PO-T2T(1:1, x nm)/$Ir(tptpy)_2(acac)$ (0.06 nm)/mCBP:PO-T2T(1:1, 16 – x nm)/POT2T (45 nm)/LiF (1 nm)/Al, where x varies from 0 to 16 nm to change the position of the non-doped yellow phosphor ultrathin layer (Fig. S7a). As shown in Fig. S7b, the ratio of the yellow emission peak intensity to the blue intensity (478 nm) as a function of the position of yellow ultrathin layer at a driving voltage of 4 V is given. As shown in Fig. S7b, the uniform intensity distribution in a wide range of regions from about 1 to 15 nm is clealy observed. This implies that the excitons are formed in a very wide region in the blue EML, which further demonstrates that all generated excitons in our present devices can be effectively confined into the blue emissive layer and provides the possibility of nearly 100% exciton utilization indirectly.